

Supporting Information

## Tuning inter-molecular charge transfer, second-order nonlinear optical and absorption spectra properties of $\pi$ -dimer under the external electric field

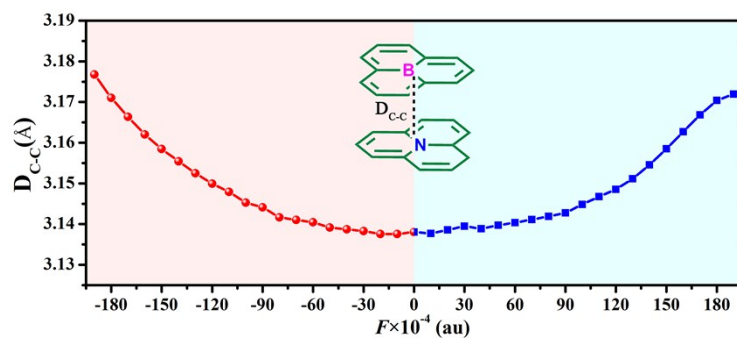
Feng-Wei Gao, Hong-Liang Xu\* and Zhong-Min Su\*

Institute of Functional Material Chemistry, National & Local United Engineering Laboratory for Power Batteries, Department of Chemistry, Northeast Normal University, Changchun 130024, People's Republic of China.

E-mail: [hlxu@nenu.edu.cn](mailto:hlxu@nenu.edu.cn), [zmsu@nenu.edu.cn](mailto:zmsu@nenu.edu.cn)

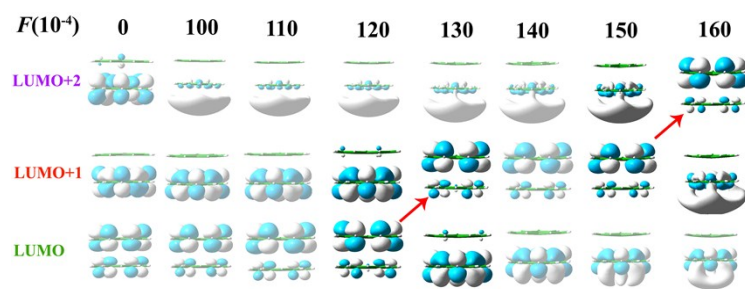
### Table of Contents

1. Evolutions of the distances between the boron and nitrogen atoms ( $D$ , [Å]) of BN-PLY<sub>2</sub> under the  $F$  ( $F = 1 \times 10^{-4}$  au) in **Figure S1**. S1
2. Evolutions of frontier molecular orbital (FMO) of BN-PLY<sub>2</sub> under the  $F$  along direction of positive z-axis in **Figure S2**. S2
3. Evolutions of the interaction energy ( $E_{\text{int}}$ , kcal mol<sup>-1</sup>) of BN-PLY<sub>2</sub> under the  $F$  ( $F = 1 \times 10^{-4}$  au) in **Figure S3**. S3
4. The first hyperpolarizabilities ( $\beta_{\text{tot}}$ , au) and the components of first hyperpolarizabilities for  $\pi$ -dimers under the  $F$  ( $F = 1 \times 10^{-4}$  au) by using the M06-2X method with different basis sets (6-31+G\*\*, 6-31+G\*, 6-31++G\*\* and 6-311+G\*\*) in **Table S1**. S4
5. The first hyperpolarizabilities ( $\beta_{\text{tot}}$ , au) and the components of first hyperpolarizabilities for BN-PLY<sub>2</sub> under the  $F$  ( $F = 1 \times 10^{-4}$  au) at the M06-2X/6-31+G\*\* level in **Table S2**. S5



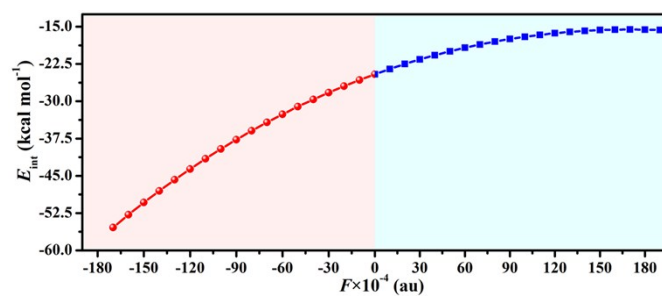
**Figure S1.** Evolutions of the distances between the boron and nitrogen atoms ( $D$ , [Å]) of PLY<sub>2</sub>-BN under the  $F$  ( $F = 1 \times 10^{-4}$  au).

Figure S1 presents the evolution of the distance between the boron and nitrogen atoms with the different strength of external electric fields. Obviously, the change trend of distances with  $F$  along direction of negative  $z$ -axis is consistent with the distances with  $F$  along direction of positive  $z$ -axis, and they are gradually increased.



**Figure S2.** Evolutions of frontier molecular orbital (FMO) of BN-PLY<sub>2</sub> under the  $F$  along direction of positive  $z$ -axis ( $F = 1 \times 10^{-4}$  au).

Figure S2 shows that the evolutions of the lowest unoccupied molecular orbital (LUMO) under the  $F$ . When the  $F_{+z}$  ranging from 120 to  $130 \times 10^{-4}$  au, the LUMO and the LUMO +1 takes place orbital interchange. When  $F$  continues to increase from  $150 \times 10^{-4}$  to  $160 \times 10^{-4}$  au, LUMO+1 and LUMO +2 exhibit orbital interchange in  $\pi$ -dimer, corresponding evolutions of FMOs of BN-PLY<sub>2</sub> under the  $F$  are presented in Figure S2.



**Figure S3.** Evolutions of the interaction energy ( $E_{\text{int}}$ , kcal mol $^{-1}$ ) of BN-PLY $_2$  under the  $F$  ( $F = 1 \times 10^{-4}$  au) by using the M06-2X with D3 method.

The dispersion-corrected is very important for evaluating interactions of  $\pi$ -dimer systems. Therefore, we use M06-2X-D3 method to calculate interaction energy ( $E_{\text{int}}$ , kcal mol $^{-1}$ ) of BN-PLY $_2$  in Figure S3. It can be clearly seen that tend of the  $E_{\text{int}}$  values calculated by using the M06-2X-D3 method are consistent with that of the M06-2X method, and the  $E_{\text{int}}$  value with the M06-2X-D3 method increase of above 1.5 kcal mol $^{-1}$  compared to M06-2X method.

**Table S1.** The first hyperpolarizabilities ( $\beta_{\text{tot}}$ , au) and the components of first hyperpolarizabilities for  $\pi$ -dimers under the  $F$  ( $F = 1 \times 10^{-4}$  au) by using the M06-2X method with different basis sets (6-31+G\*\*, 6-31+G\*, 6-31++G\*\* and 6-311+G\*\*).

<b>Basis set</b>		<b>-190</b>	<b>-150</b>	<b>-100</b>	<b>-50</b>	<b>0</b>	<b>50</b>	<b>100</b>	<b>150</b>	<b>190</b>
6-31+G**	$\beta_x$	12.85	7.05	1.22	-2.53	-7.22	-6.70	-6.33	-1.74	0.31
	$\beta_y$	1.80	-1.55	-5.96	-8.32	3.07	-10.70	-8.78	7.17	26.94
	$\beta_z$	$4.07 \times 10^3$	$3.24 \times 10^3$	$2.85 \times 10^3$	$2.85 \times 10^3$	$3.02 \times 10^3$	$3.00 \times 10^3$	$2.05 \times 10^3$	$-9.14 \times 10^2$	$-6.67 \times 10^3$
	$\beta_{\text{tot}}$	$4.07 \times 10^3$	$3.24 \times 10^3$	$2.85 \times 10^3$	$2.85 \times 10^3$	$3.02 \times 10^3$	$3.00 \times 10^3$	$2.05 \times 10^3$	$9.14 \times 10^2$	$6.67 \times 10^3$
6-31+G*	$\beta_x$	12.52	6.86	1.10	-2.55	-5.98	-6.57	-6.21	-1.79	0.16
	$\beta_y$	1.66	-1.43	-5.50	-7.46	3.01	-9.29	-7.55	7.69	26.71
	$\beta_z$	$4.10 \times 10^3$	$3.26 \times 10^3$	$2.86 \times 10^3$	$2.86 \times 10^3$	$3.04 \times 10^3$	$3.01 \times 10^3$	$2.05 \times 10^3$	$-9.13 \times 10^2$	$-6.67 \times 10^3$
	$\beta_{\text{tot}}$	$4.10 \times 10^3$	$3.26 \times 10^3$	$2.86 \times 10^3$	$2.86 \times 10^3$	$3.04 \times 10^3$	$3.01 \times 10^3$	$2.05 \times 10^3$	$9.13 \times 10^2$	$6.67 \times 10^3$
6-31++G**	$\beta_x$	12.75	6.65	1.08	-2.54	-7.22	-6.74	-6.46	-1.42	1.79
	$\beta_y$	3.40	-1.73	-6.25	-8.36	3.03	-10.88	-9.21	7.78	31.86
	$\beta_z$	$4.29 \times 10^3$	$3.34 \times 10^3$	$2.87 \times 10^3$	$2.83 \times 10^3$	$2.98 \times 10^3$	$2.93 \times 10^3$	$1.95 \times 10^3$	$-1.07 \times 10^3$	$-6.90 \times 10^3$
	$\beta_{\text{tot}}$	$4.29 \times 10^3$	$3.34 \times 10^3$	$2.87 \times 10^3$	$2.83 \times 10^3$	$2.98 \times 10^3$	$2.93 \times 10^3$	$1.95 \times 10^3$	$1.07 \times 10^3$	$6.90 \times 10^3$
6-311+G**	$\beta_x$	10.95	6.42	0.90	-3.02	-6.44	-7.35	-6.84	-1.81	0.52
	$\beta_y$	-2.29	-4.95	-7.52	-8.33	3.60	-10.29	-11.27	-3.70	3.33
	$\beta_z$	$3.59 \times 10^3$	$2.96 \times 10^3$	$2.73 \times 10^3$	$2.80 \times 10^3$	$3.01 \times 10^3$	$2.99 \times 10^3$	$2.10 \times 10^3$	$-7.02 \times 10^2$	$-6.56 \times 10^3$
	$\beta_{\text{tot}}$	$3.59 \times 10^3$	$2.96 \times 10^3$	$2.73 \times 10^3$	$2.80 \times 10^3$	$3.01 \times 10^3$	$2.99 \times 10^3$	$2.10 \times 10^3$	$7.02 \times 10^2$	$6.56 \times 10^3$

We used the M06-2X results to further evaluate the effect of the different basis sets on the second-order NLO properties, so four basis sets (6-31+G\*, 6-31+G\*\*, 6-31++G\*\*, and 6-311+G\*\*) were chosen to calculate the  $\beta_{\text{tot}}$  value under the  $F$ . Obviously, the different basis sets obtain the same trend in the  $\beta_{\text{tot}}$  value, and the  $\beta_{\text{tot}}$  values are very close. The above results confirm the reliability and accuracy of 6-31+G\*\* basis set.

**Table S2.** The first hyperpolarizabilities ( $\beta_{\text{tot}}$ , au) and the components of first hyperpolarizabilities for  $\pi$ -dimers under the  $F$  ( $F = 1 \times 10^{-4}$  au) at the M06-2X/6-31+G\*\* level.

	$\beta_x$	$\beta_y$	$\beta_z$	$\beta_{\text{tot}}$
<b>-190</b>	12.85	1.80	$4.07 \times 10^3$	$4.07 \times 10^3$
<b>-150</b>	7.05	-1.55	$3.24 \times 10^3$	$3.24 \times 10^3$
<b>-100</b>	1.22	-5.96	$2.85 \times 10^3$	$2.85 \times 10^3$
<b>-50</b>	-2.53	-8.32	$2.85 \times 10^3$	$2.85 \times 10^3$
<b>0</b>	-7.22	3.07	$3.02 \times 10^3$	$3.02 \times 10^3$
<b>50</b>	-6.70	-10.70	$3.00 \times 10^3$	$3.00 \times 10^3$
<b>100</b>	-6.33	-8.78	$2.05 \times 10^3$	$2.05 \times 10^3$
<b>150</b>	-1.74	7.17	$-9.14 \times 10^2$	$9.14 \times 10^2$
<b>190</b>	0.31	26.94	$-6.67 \times 10^3$	$6.67 \times 10^3$

Table S2 results show that the  $\beta_z$  values are very close to the  $\beta_{\text{tot}}$  values under the  $F$ , indicating that the greatest contribution to the  $\beta_{\text{tot}}$  is the  $\beta_z$  value for  $\pi$ -dimer.